

Research Article

Synthesis, Spectroscopic Characterization, Structural Studies, and *In Vitro* Antitumor Activities of Pyridine-3-carbaldehyde Thiosemicarbazone Derivatives

Wilfredo Hernández ¹, Fernando Carrasco ¹, Abraham Vaisberg ²,
Evgenia Spodine ³, Jorge Manzur,⁴ Maik Icker ⁵, Harald Krautscheid ⁵,
and Lothar Beyer⁵

¹Facultad de Ingeniería y Arquitectura, Universidad de Lima, Av. Javier Prado Este 4600, Lima 33, Peru

²Laboratorio de Investigación y Desarrollo, Facultad de Ciencias y Filosofía, Universidad Peruana Cayetano Heredia, Av. Honorio Delgado 430, Lima 31, Peru

³Facultad de Ciencias Químicas y Farmacéuticas, Universidad de Chile, CEDENNA, Olivos 1007, Casilla 233, Independencia, 8330492 Santiago, Chile

⁴Facultad de Ciencias Físicas y Matemáticas, Universidad de Chile, Av. Beauchef 850, 8320198 Santiago, Chile

⁵Fakultät für Chemie und Mineralogie, Universität Leipzig, Johannisallee 29, D-04103 Leipzig, Germany

Correspondence should be addressed to Wilfredo Hernández; whernandez79@yahoo.es, Evgenia Spodine; espodine@ciq.uchile.cl, and Maik Icker; maik.icker@uni-leipzig.de

Received 20 June 2020; Revised 28 July 2020; Accepted 31 July 2020; Published 14 September 2020

Academic Editor: João Paulo Leal

Copyright © 2020 Wilfredo Hernández et al. This is an open access article distributed under the Creative Commons Attribution License, which permits unrestricted use, distribution, and reproduction in any medium, provided the original work is properly cited.

Eight new thiosemicarbazone derivatives, 6-(1-trifluoroethoxy)pyridine-3-carbaldehyde thiosemicarbazone (**1**), 6-(4'-fluorophenyl)pyridine-3-carbaldehyde thiosemicarbazone (**2**), 5-chloro-pyridine-3-carbaldehyde thiosemicarbazone (**3**), 2-chloro-5-bromo-pyridine-3-carbaldehyde thiosemicarbazone (**4**), 6-(3',4'-dimethoxyphenyl)pyridine-3-carbaldehyde thiosemicarbazone (**5**), 2-chloro-5-fluor-pyridine-3-carbaldehyde thiosemicarbazone, (**6**), 5-iodo-pyridine-3-carbaldehyde thiosemicarbazone (**7**), and 6-(3',5'-dichlorophenyl)pyridine-3-carbaldehyde thiosemicarbazone (**8**) were synthesized, from the reaction of the corresponding pyridine-3-carbaldehyde with thiosemicarbazide. The synthesized compounds were characterized by ESI-Mass, UV-Vis, IR, and NMR (¹H, ¹³C, ¹⁹F) spectroscopic techniques. Molar mass values and spectroscopic data are consistent with the proposed structural formulas. The molecular structure of **7** has been also confirmed by single crystal X-ray diffraction. In the solid state **7** exists in the *E* conformation about the N2-N3 bond; **7** also presents the *E* conformation in solution, as evidenced by ¹H NMR spectroscopy. The *in vitro* antitumor activity of the synthesized compounds was studied on six human tumor cell lines: H460 (lung large cell carcinoma), HuTu80 (duodenum adenocarcinoma), DU145 (prostate carcinoma), MCF-7 (breast adenocarcinoma), M-14 (amelanotic melanoma), and HT-29 (colon adenocarcinoma). Furthermore, toxicity studies in 3T3 normal cells were carried out for the prepared compounds. The results were expressed as IC₅₀ and the selectivity index (SI) was calculated. Biological studies revealed that **1** (IC₅₀ = 3.36 to 21.35 μM) displayed the highest antiproliferative activity, as compared to the other tested thiosemicarbazones (IC₅₀ = 40.00 to >582.26 μM) against different types of human tumor cell lines. **1** was found to be about twice as cytotoxic (SI = 1.82) than 5-fluorouracile (**5-FU**) against the M14 cell line, indicating its efficiency in inhibiting the cell growth even at low concentrations. A slightly less efficient activity was shown by **1** towards the HuTu80 and MCF7 tumor cell lines, as compared to that of **5-FU**. Therefore, **1** can be considered as a promising candidate to be used as a pharmacological agent, since it presents significant activity and was found to be more innocuous than the **5-FU** anticancer drug against the 3T3 mouse embryo fibroblast cells.

1. Introduction

For several years, thiosemicarbazones with general formula $R^1R^2CH=N-NH-(C=S)-NH_2$ have been attracting the attention of researchers, not only because of their multi-functional coordination modes to transition metal ions [1, 2], but also because of their wide range of biological properties including antibacterial [3–6], antifungal [7], antimycobacterium tuberculosis [8, 9], and antitumoral [10–14] activity.

Thiosemicarbazones usually react as chelating ligands with metal ions by bonding through the thiocarbonyl sulfur and the azomethine nitrogen atoms [15–17]. In addition to this, thiosemicarbazones and the corresponding coordination compounds have been extensively investigated for their antiproliferative activity against different human tumor cell lines. It has been shown that the mechanism of antitumoral action of α -(*N*)-heterocyclic thiosemicarbazones is due to its ability to inhibit the enzyme ribonucleotide diphosphate reductase, which catalyzes the conversion of ribonucleotides into deoxyribonucleotides during the DNA syntheses [18, 19].

A variety of heterocyclic thiosemicarbazones also proved to be cytotoxic against several tumor cell lines. Thus, cytotoxic studies with pyridine thiosemicarbazone derivatives: pyridine-2-carbaldehyde thiosemicarbazone, 2-acetylpyridine-4-cyclohexyl thiosemicarbazone, and 2-formylpyridin-4-*N*-ethyl-thiosemicarbazone, revealed that these compounds possess higher antiproliferative activity *in vitro* ($IC_{50} = < 0.55$ to $4.88 \mu M$) against MCF-7 (human breast cancer cell line), as compared to cisplatin ($IC_{50} = 8.0 \mu M$) [20–22].

In previous articles, we have reported the cytotoxic activity of compounds derived from benzaldehyde, naphthaldehyde, and furan-2-carbaldehyde thiosemicarbazones against different human tumor cell lines [23–25]. *In vitro* antitumor studies, against the chronic myelogenous leukemia (K562) and amelanotic melanoma (M-14) cell lines, revealed that compounds 2-hydroxynaphthaldehyde thiosemicarbazone ($IC_{50} = 0.30$ and $7.30 \mu M$, respectively) and 4-phenyl-1-(2'-hydroxynaphthaldehyde) thiosemicarbazone ($IC_{50} = 0.60$ and $6.40 \mu M$, respectively) were more cytotoxic than the corresponding naphthaldehyde thiosemicarbazone compounds ($IC_{50} = 15.00$ and $6.4 \mu M$, respectively) and 4-phenyl-1-naphthaldehyde thiosemicarbazone ($IC_{50} = 24.70$ and $>250 \mu M$, respectively) [26]. In addition, in this research compound 2-hydroxynaphthaldehyde thiosemicarbazone was found to be about four times more cytotoxic than the reference drug cisplatin against the K562 cell line.

As a part of our efforts towards the synthesis and structural characterization of new materials containing biorelevant pyridinyl thiosemicarbazones and the understanding of their cytotoxic activity against different human tumor cell lines, the present work describes the synthesis and spectral characterization of eight new pyridine-3-carbaldehyde thiosemicarbazone derivatives. Compounds **1–8** were tested for their *in vitro* antiproliferative activity against six human tumor cell lines: H460 (lung large cell carcinoma), HuTu80 (duodenum adenocarcinoma), DU145 (prostate

carcinoma), MCF-7 (breast adenocarcinoma), M-14 (amelanotic melanoma), and HT-29 (colon adenocarcinoma).

2. Materials and Methods

2.1. Chemicals and Instrumentation. All reagents and solvents were purchased from Sigma-Aldrich of analytical grade and were used without further purification. The tested human tumor cell lines were H460 (lung large cell carcinoma), HuTu80 (duodenum adenocarcinoma), DU145 (prostate carcinoma), MCF-7 (breast adenocarcinoma), M-14 (amelanotic melanoma), and HT-29 (colon adenocarcinoma), while the tested non-tumor cell line consisted of BALB/3T3 mouse embryonic fibroblast cells. Both the human tumor cell lines and the non-tumor cells were obtained from the American Type Culture Collection or from the National Cancer Institute. Cytotoxicity screening was performed using the sulforhodamine B (SRB) colorimetric assay [27].

Melting points were determined on a Büchi melting point B-545 apparatus. Elemental analyses were determined on an Elementar Vario EL analyzer. ESI-MS spectra were recorded on a Waters-Quattro Premier XE™ tandem quadrupole mass spectrometer and MicrOTOF Bruker Daltonics mass spectrometer, using methanol as the sample dissolution medium. The Infrared (IR) spectra were recorded using a Nicolet iS10 Fourier Transform Infrared (FT-IR) spectrometer equipped with an attenuated total reflectance accessory using a diamond crystal. The measurements were obtained in absorbance mode, recorded for 32 scans at a resolution of 4 cm^{-1} . All the measurements were carried out with an automatic baseline correction. The UV-VIS spectra were recorded on a Thermo Scientific Evolution 201 spectrophotometer. The ^1H (300 MHz or 400 MHz), ^{13}C (75.5 MHz or 100 MHz), and ^{19}F (376 MHz) NMR spectra were obtained on a Varian Mercury Plus 300 or Varian Mercury Plus 400 spectrometer at 299 K, using DMSO- d_6 as solvent. The chemical shifts (δ) in ppm were referenced relative to residual DMSO (2.50 ppm, ^1H ; 39.52 ppm, ^{13}C { ^1H }; ^{19}F via IUPAC Ξ -scale with respect to the ^1H reference). The splitting of proton and carbon resonances in the reported ^1H and ^{13}C NMR spectra is defined as s = singlet, d = doublet, t = triplet, q = quartet, and m = multiplet.

2.2. Experimental Procedures

2.2.1. Synthesis of the Pyridine-3-carbaldehyde Thiosemicarbazone Derivatives **1–8**.

General Method. The pyridine-2-carbaldehyde derivative (2 mmol) in 70 mL of methanol was added dropwise to a solution of the thiosemicarbazide (0.27 g, 3 mmol) in 50 mL of methanol during 30 minutes. The mixture was refluxed for 3 h under constant stirring. Then, this liquid was stirred for 24 h at room temperature. The final mixture was filtered and the filtrate was concentrated to half the volume under reduced pressure. After a slow evaporation of the concentrate at room temperature, a solid product was obtained. It was filtered, washed several times with cold ethanol and

dried *in vacuo*. Recrystallization of the solids was performed from hot acetone.

6-(1-Trifluoroethoxy)pyridine-3-carbaldehyde Thiosemicarbazone (1). Colorless solid. Yield 68%, m.p. 210–212°C. Anal. Cal. for C₉H₉ON₄SF₃ (278.25 g/mol): C, 38.85; H, 3.26; N, 20.14. Found: C, 38.92; H, 2.51; N, 20.75. ESI-MS: *m/z* 279.05 [M + H]⁺, 301.04 [M + Na]⁺. UV-VIS [DMSO, λ_{max}.(nm)] 317. IR (KBr): ν = 3451, 3294 (NH₂), 3154 (NHCS), 1610 (CH=N), 1536 (C=N), 1059 (N-N), 865 (C=S) cm⁻¹. ¹H-NMR (300 MHz, *d*₆-DMSO, ppm): δ 5.02 (*q*, 2H, OCH₂CF₃, *J* = 9.1 Hz), 8.20 and 8.08 (*s*, 2H, NH₂), 8.46 (*d*, 1H: H², Py, *J* = 2.3 Hz), 8.41 (*dd*, 1H: H⁴, Py, *J* = 8.6, 2.3 Hz), 7.03 (*d*, 1H: H⁵, Py, *J* = 8.6 Hz), 8.03 (*s*, 1H, CH=N), 11.49 (*s*, =N-NH). ¹³C-NMR (75 MHz, *d*₆-DMSO): δ 61.59 (*q*, OCH₂CF₃, *J* = 34.6 Hz), 124.04 (*q*, CF₃, *J* = 277.6 Hz); 161.87, 146.81, 137.64, 125.88, 111.14 (Py); 138.80 (HC=N); 178.04 (C=S). ¹⁹F{¹H}-NMR (376 MHz, *d*₆-DMSO): -72.85 (CF₃).

6-(4-Fluorophenyl)pyridine-3-carbaldehyde Thiosemicarbazone (2). Colorless solid. Yield 65%, m.p. 241–243°C. Anal. Cal. for C₁₃H₁₁N₄SF (274.32 g/mol): C, 56.92; H, 4.04; N, 20.42. Found: C, 56.94; H, 3.14; N, 20.79. ESI-MS: *m/z* 275.08 [M + H]⁺. UV-VIS [DMSO, λ_{max}.(nm)] 248, 323. IR (KBr): ν = 3422, 3273 (NH₂), 3078 (NHCS), 1633 (CH=N), 1525 (C=N), 1093 (N-N), 833 (C=S) cm⁻¹. ¹H-NMR (400 MHz, -*d*₆-DMSO, ppm): δ 7.86 (*t*, 2H: H^{2'}, H^{6'}, 4-*F*-Ph, *J* = 8.9, 5.4 Hz), 7.34 (*t*, 2H: H^{3'}, H^{5'}, 4-*F*-Ph, *J* = 8.9 Hz), 8.33 and 8.28 (*s*, 2H, NH₂), 8.57 (*t*, 1H: H⁴, Py, *J* = 2.1 Hz), 8.85 (*dd*, 1H: H⁵, Py, *J* = 4.9, 2.1 Hz), 8.14 (*s*, 1H, CH=N), 11.64 (*s*, 1H, =N-NH). ¹³C-NMR (100 MHz, *d*₆-DMSO, ppm): δ 162.41 (*d*, F-C^{4'}, *J* = 245.5 Hz), 133.02 (*d*, *J* = 3.3 Hz), 129.27 (*d*, *J* = 8.4 Hz), 115.91 (*d*, *J* = 21.5 Hz) (4-*F*-Ph); 148.28, 147.86, 134.43, 131.05, 130.31 (Py); 138.98 (HC=N); 178.28 (C=S). ¹⁹F{¹H}-NMR (376 MHz, *d*₆-DMSO): -114.54 (F-Ph).

5-Chloro-pyridine-3-carbaldehyde Thiosemicarbazone (3). Colorless solid. Yield 56%. m.p. 240–241°C. Anal. Cal. for C₇H₇N₄SCl (214.68 g/mol): C, 39.16; H, 3.29; N, 26.10. Found: C, 39.09; H, 2.50; N, 26.66. ESI-MS: *m/z* 215.02 [M + H]⁺, 236.99 [M + Na]⁺. UV-VIS [DMSO, λ_{max}.(nm)] 324. IR (KBr): ν = 3324 (NH₂), 3120 (NHCS), 1629 (CH=N), 1525 (C=N), 1096 (N-N), 843 (C=S) cm⁻¹. ¹H-NMR (300 MHz, *d*₆-DMSO, ppm): δ 8.04 (*s*, 1H: H⁴, Py), 8.79 (*s*, 1H: H⁶, Py), 8.33 (*s*, 2H, NH₂), 8.57 (*s*, 1H, CH=N), 11.66 (*s*, 1H, =N-NH). ¹³C-NMR (75 MHz, *d*₆-DMSO, ppm): δ 149.00, 147.77, 133.09, 132.42, 132.04, (Py); 137.79 (HC=N); 178.85 (C=S). (5) **2-Chloro-5-bromo-pyridine-3-carbaldehyde Thiosemicarbazone (4).** Yellow solid. Yield 70%. m.p. 135–137°C. Anal. Cal. for C₇H₆N₄SBrCl (293.57 g/mol): C, 28.64; H, 2.06; N, 19.08. Found: C, 28.75; H, 1.82; N, 19.31. ESI-MS: *m/z* 292.93, 294.93 [M + H]⁺. UV-VIS [DMSO, λ_{max}.(nm)] 335. IR (KBr): ν = 3446, 3238 (NH₂), 3146

(NHCS), 1602 (CH=N), 1536 (C=N), 1061 (N-N), 837 (C=S) cm⁻¹. ¹H-NMR (300 MHz, *d*₆-DMSO, ppm): δ 9.02 (*d*, 1H⁴, Py, *J* = 3.0 Hz), 8.53 (*d*, 1H⁶, Py, *J* = 3.0 Hz), 8.45 (*s*, 2H, NH₂), 8.28 (*s*, 1H, CH=N), 11.77 (*s*, 1H, =N-NH). ¹³C-NMR (75 MHz, *d*₆-DMSO, ppm): δ 150.87, 148.22, 135.73, 130.78, 120.24 (Py); 138.24 (HC=N); 178.96, 171.65 (C=S).

6-(3,4-Dimethoxyphenyl)pyridine-3-carbaldehyde Thiosemicarbazone (5). Yellow solid. Yield 70%, m.p. 219–221°C. Anal. Cal. for C₁₅H₁₆O₂N₄S (316.38 g/mol): C, 56.94; H, 5.10; N, 17.71. Found: C, 56.81; H, 4.80; N, 17.54. ESI-MS: *m/z* 317.11 [M + H]⁺. UV-VIS [DMSO, λ_{max}.(nm)] 351. IR (KBr): ν = 3375, 3269 (NH₂), 3116 (NHCS), 1587 (CH=N), 1531 (C=N), 1018 (N-N), 832 (C=S) cm⁻¹. ¹H-NMR (300 MHz, *d*₆-DMSO, ppm): δ 3.81, 3.86 (*s*, 3H, CH₃O-Ph), 7.98 (*d*, 1H: H², Ph, *J* = 9.0 Hz), 7.06 (*d*, 1H: H⁵, Ph, *J* = 9.0 Hz), 7.74 (*s*, 1H: H⁶, Ph); 8.15 and 8.28 (*s*, 2H, NH₂); 8.90 (*s*, 1H: H², Py), 7.72 (*d*, 1H: H⁴, Py, *J* = 9.0 Hz), 8.34 (*d*, 1H: H⁵, Py, *J* = 12.0 Hz); 8.09 (*s*, 1H, CH=N), 11.58 (*s*, 1H, =N-NH). ¹³C-NMR (75 MHz, *d*₆-DMSO, ppm): δ 149.25, 139.71, 131.17, 119.81, 112.16, 110.29 (Ph); 156.81, 150.55, 134.93, 128.61, 119.97 (Py); 149.40 (HC=N); 178.54 (C=S).

2-Chloro-5-fluor-pyridine-3-carbaldehyde Thiosemicarbazone (6). Colorless solid. Yield 82%. m.p. 139–140°C. Anal. Cal. for C₇H₆N₄SFCl (232.67 g/mol): C, 36.13; H, 2.60; N, 24.08. Found: C, 36.15; H, 2.23; N, 24.44. ESI-MS: *m/z* 230.91 [M - H]⁻. UV-VIS [DMSO, λ_{max}.(nm)] 250, 334. IR (KBr): ν = 3457, 3290 (NH₂), 3158 (NHCS), 1605 (CH=N), 1525 (C=N), 1067 (N-N), 840 (C=S) cm⁻¹. ¹H-NMR (400 MHz, *d*₆-DMSO, ppm): δ 8.75 (*dd*, 1H: H⁴, Py, *J* = 9.5, 3.0 Hz), 8.45 (*d*, 1H: H⁶, Py, *J* = 3.0 Hz); 8.43 and 8.40 (*s*, 2H, NH₂); 8.30 (*s*, 1H, CH=N), 11.79 (*s*, 1H, =N-NH). ¹³C-NMR (100 MHz, *d*₆-DMSO, ppm): δ 158.82 (*d*, *J* = 253.4 Hz), 143.84 (*d*, *J* = 1.8 Hz), 138.27 (*d*, *J* = 26.8 Hz), 130.37 (*d*, *J* = 5.3 Hz), 122.57 (*d*, *J* = 22.2 Hz) (Py); 135.48 (*d*, HC=N, *J* = 2.0 Hz); 178.98 (C=S). ¹⁹F{¹H}-NMR (376 MHz, *d*₆-DMSO): -129.36 (F-Py).

5-Iodo-pyridine-3-carbaldehyde Thiosemicarbazone (7). Colorless solid. Yield 69%. m.p. 242–244°C. MW: C₇H₇N₄SI (306.13 g/mol), ESI-MS: *m/z* 305.00 [M - H]⁻. UV-VIS [DMSO, λ_{max}.(nm)] 267, 325. IR (KBr): ν = 3370, 3225 (NH₂), 3147 (NHCS), 1683 (CH=N), 1593 (C=N), 1015 (N-N), 867 (C=S) cm⁻¹. ¹H-NMR (400 MHz, *d*₆-DMSO, ppm): δ 8.79, (*d*, 1H, Py, *J* = 1.7 Hz), 8.75–8.76 (*m*, 2H, Py); 8.27 (*s*, 2H, NH₂); 7.97 (*s*, 1H, CH=N); 11.62 (*s*, 1H, =N-NH). ¹³C-NMR (100 MHz, *d*₆-DMSO, ppm): δ 155.75, 147.76, 141.25, 132.44, 94.95 (Py); 138.0 (HC=N); 178.48 (C=S).

6-(3,5-Dichlorophenyl)pyridine-3-carbaldehyde Thiosemicarbazone (8). Colorless solid. Yield 90%. m.p. 223–225°C. MW: C₁₃H₁₀N₄SCl₂ (325.22 g/mol), ESI-MS: *m/z* 324.91 [M - H]⁻. UV-VIS [DMSO, λ_{max}.(nm)] 340. IR (KBr): ν = 3356, 3256 (NH₂), 3160 (NHCS),

1600 (CH=N), 1532 (C=N), 1105 (N-N), 804 (C=S) cm^{-1} . $^1\text{H-NMR}$ (400 MHz, d_6 -DMSO, ppm): δ 8.43 (d, 2H: H^2 , H^5 , Ph, $J = 6.0$ Hz), 7.68 (s, 1H: H^4 , Ph); 8.98 (s, 1H: H^2 , Py), 8.11 (s, 1H: H^4 , Py, $J = 6.0$ Hz), 8.14 (d, 1H: H^5 , Py, $J = 6.0$ Hz); 8.31 and 8.22 (s, 2H, NH_2); 8.17 (s, 1H, CH=N), 11.64 (s, 1H, =N-NH). $^{13}\text{C-NMR}$ (100 MHz, d_6 -DMSO, ppm): δ 139.07, 135.22, 125.58 (Ph); 153.65, 149.46, 130.65, 129.04, 121.28 (Py); 141.91 (HC=N); 178.70 (C=S).

2.2.2. Crystal Structure Determination. Data were collected at 180 K using a STOE StadiVari diffractometer equipped with a copper X-ray microsource (Cu $K\alpha$ radiation) and a Dectris Pilatus 300 K detector. All data were corrected for Lorentz and polarization effects; absorption effects were corrected based on numerical absorption corrections. In addition, a scaling correction was performed using Stoe X-Area software [28]. The structure of **7** was solved by direct methods (ShelxS) and refined using the full-matrix least-squares method against F^2 (ShelxL) [29]. Diagrams of the molecular structure showing thermal ellipsoids with 50% probability were generated using Diamond3 software [30].

2.2.3. Biological Activity.

Cell Culture. BALB/3T3 cells were maintained in Dulbecco's modified Eagle's medium (DMEM) supplemented with 10% calf serum and 50 $\mu\text{g}/\text{mL}$ gentamycin. H460, HuTu80, and DU145 were maintained in minimal essential medium (MEM) supplemented with 10% fetal bovine serum and 50 $\mu\text{g}/\text{mL}$ gentamycin. MCF-7 and HT-29 were maintained in RPMI 1640 supplemented with 7.5% fetal bovine serum and 50 $\mu\text{g}/\text{mL}$ gentamycin. Cells were grown at 37°C in a 5% CO_2 humidified environment.

Assessment of Cytotoxicity. *In vitro* cytotoxic activity of the prepared compounds was tested using the sulforhodamine B (SRB) assay [27]. Briefly, cells were seeded onto 96-well plates at a density of 3000–5000 cells per well and incubated at 37°C, 5% CO_2 , 95% air and 95% relative humidity, with their corresponding growth medium for 24 h to allow for cell attachment. Solutions of the pyridine-3-carbaldehyde thiosemicarbazone derivatives in DMSO at different concentrations (1.95, 7.81, 31.25, and 125 $\mu\text{g}/\text{mL}$) and solutions of 5-fluorouracil in DMSO at different concentrations (0.061, 0.244, 0.977, and 3.91 $\mu\text{g}/\text{mL}$) were added to the different cell lines and incubated for 48 h at 37°C in 5% CO_2 humidified atmosphere. After 48 h, cells were treated with trichloroacetic acid (TCA), washed, dried, and stained with a solution of 0.4% sulforhodamine B in 1% acetic acid for 20 minutes. Excess stain was washed out four times with 1% acetic acid. After complete drying, the bound dye was solubilized with 10 mM Tris buffer (pH 10.5) and color intensity was measured on an automated plate reader at a wavelength of 510 nm. The IC_{50} value was defined as the concentration of test sample resulting in a 50% reduction of absorbance as compared with untreated controls, i.e.,

50% reduction in the growth of the cells, and was determined by linear regression analysis.

3. Results and Discussion

3.1. Synthesis and Characterization. Pyridine-3-carbaldehyde thiosemicarbazone derivatives **1–8** were prepared by condensing the thiosemicarbazide with a wide range of substituted pyridine 3-carbaldehydes, according to a literature procedure [24, 25], as shown in Scheme 1.

All the new synthesized compounds were obtained in good yields (56–90%) and were satisfactorily characterized by elemental analysis, ESI-Mass, UV-Vis (ultraviolet-visible), FT-IR, and (^1H , ^{13}C , ^{19}F) nuclear magnetic resonance spectroscopy. The isolated compounds are soluble in common organic solvents, such as dichloromethane, chloroform, acetone, dimethylformamide, and dimethylsulphoxide.

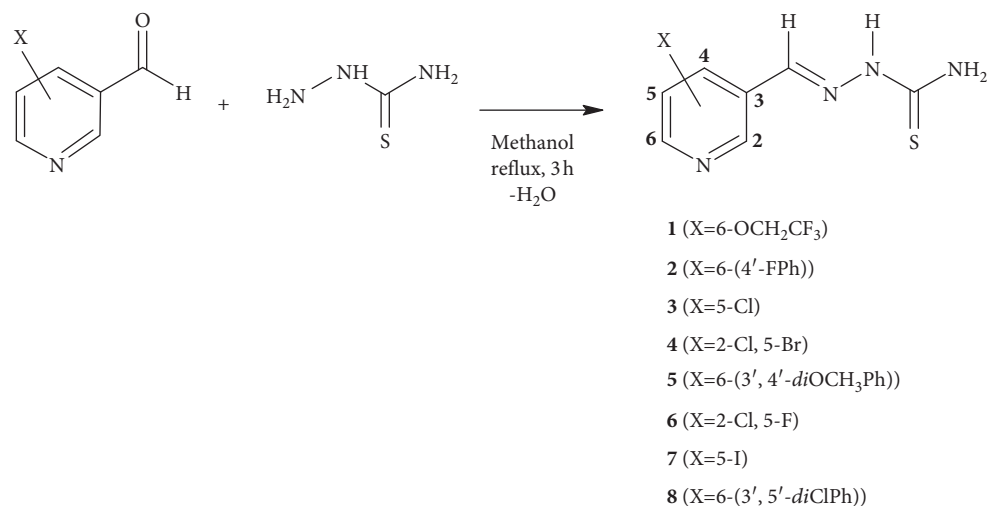
The mass and spectroscopic data obtained for all the thiosemicarbazone derivatives are in agreement with the proposed structures and are given as Supplementary Material.

3.1.1. Infrared Spectra. The corresponding FT-IR spectra of the studied compounds are given as Supplementary Material (Figures S1–S8). In the FT-IR spectra of all eight compounds, the broad bands observed in the ranges of 3457–3225 and 3158–3078 cm^{-1} were assigned to the $\nu(\text{NH}_2)$ and $\nu(\text{NHCS})$ vibrations, respectively [31, 32]. The strong and medium absorption bands at 1587–1683 cm^{-1} were attributed to the (CH=N) stretching vibrations of the imine group, which is in agreement with the vibrations found for other thiosemicarbazone derivatives [31]. The strong bands of the pyridine C=N group were observed at 1593–1525 cm^{-1} , while the bands in the 1096–1015 cm^{-1} region were assigned to the $\nu(\text{N-N})$ vibrations. In all FT-IR spectra, a peak around 2500 cm^{-1} attributed to the SH group was not observed; the medium bands which are in 867–804 cm^{-1} range were ascribed to (C=S) stretching vibrations, indicating that the studied compounds are present in the thione form [33, 34].

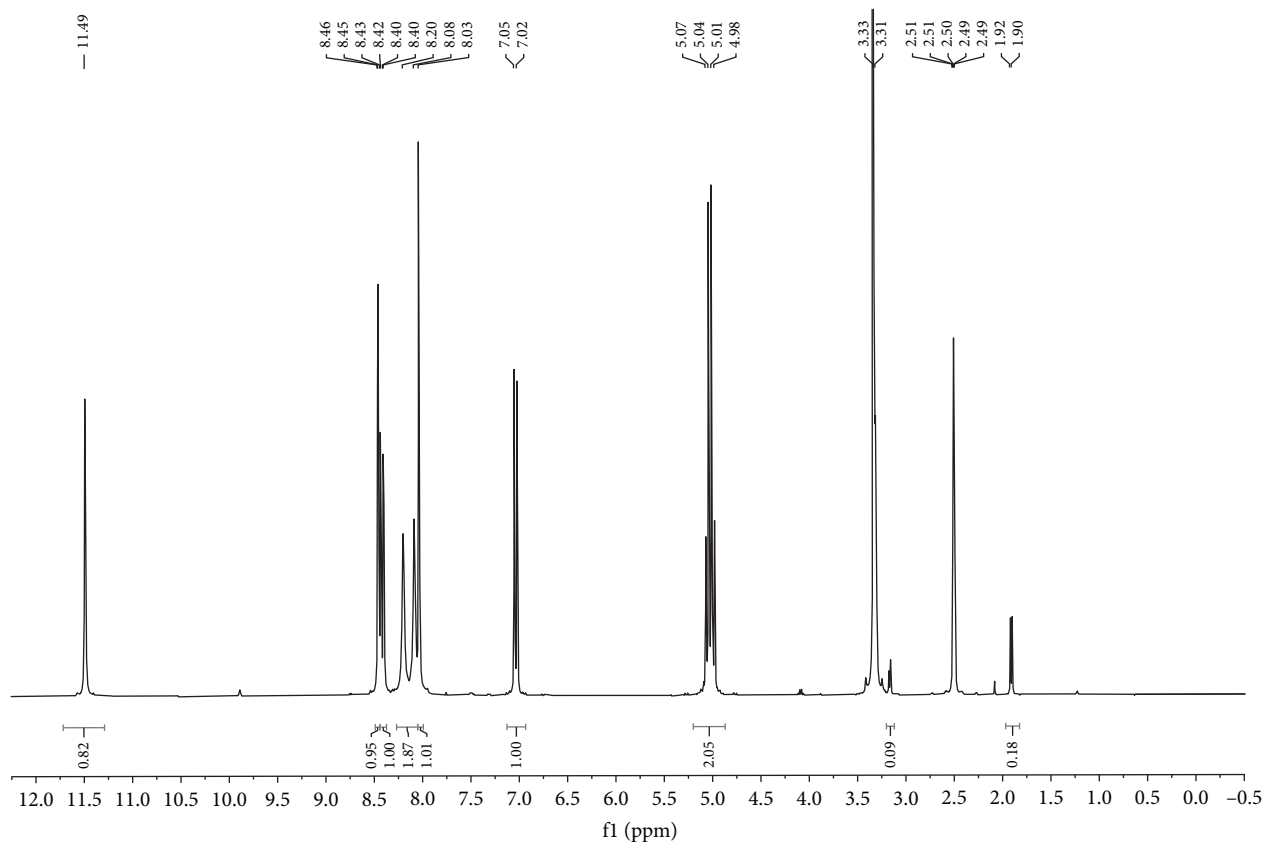
3.1.2. Mass Spectra. The mass spectra of all thiosemicarbazones show the molecular ion peaks ($[\text{M} + \text{H}]^+$ or $[\text{M} - \text{H}]^+$) corresponding to the respective molecular masses $[\text{M}]$ of the prepared compounds. For **4**, two peaks were observed at $m/z = 292.93$ and 294.94, respectively, due to the presence of ^{79}Br and ^{81}Br isotopes.

3.1.3. NMR Spectra. The NMR spectra of the compounds were recorded in DMSO- d_6 solution in order to confirm the presence of the functional groups and proposed molecular formulas. The ^1H resonances were assigned on the basis of chemical shifts, multiplicities, and coupling constants and, in some cases, by 2D NMR data. The $^1\text{H-NMR}$, ^{13}C NMR, and ^{19}F NMR spectra of **1** are shown in Figures 1–3.

All $^1\text{H-NMR}$ spectra of compounds **1–8** showed a singlet in the region $\delta = 11.79 - 11.49$ for the =N-NH



SCHEME 1: Synthesis of pyridine-3-carbaldehyde thiosemicarbazone derivatives.

FIGURE 1: ¹H-NMR spectrum of compound 1.

proton [35]. These results are similar to the chemical shifts found for compound 4-phenyl-1-benzaldehyde thiosemicarbazone ($\delta=11.83$), which exists in the *E* isomeric form [23]. The signal of the imine-CH=N proton appeared as a singlet at $\delta=8.57-7.97$ [36]. The NH₂ protons of the thioamide group showed broad peaks at $\delta=8.45-8.08$ [23]. On the other hand, the resonance lines of the protons corresponding to the pyridine ring

were observed at $\delta=9.02-7.05$, in agreement with the chemical shifts found for other compounds derived from pyridine-2-carbaldehyde thiosemicarbazone [33, 37]. For compounds 2, 5, and 8, the aromatic proton signals of the phenyl fragment bound to the pyridine ring were affected by the presence of the *fluoro*, *methoxy*, and *chloro* substituents in the C-4', C-3',4', and C-3',5' positions, respectively. These signals are deshielded for the protons in

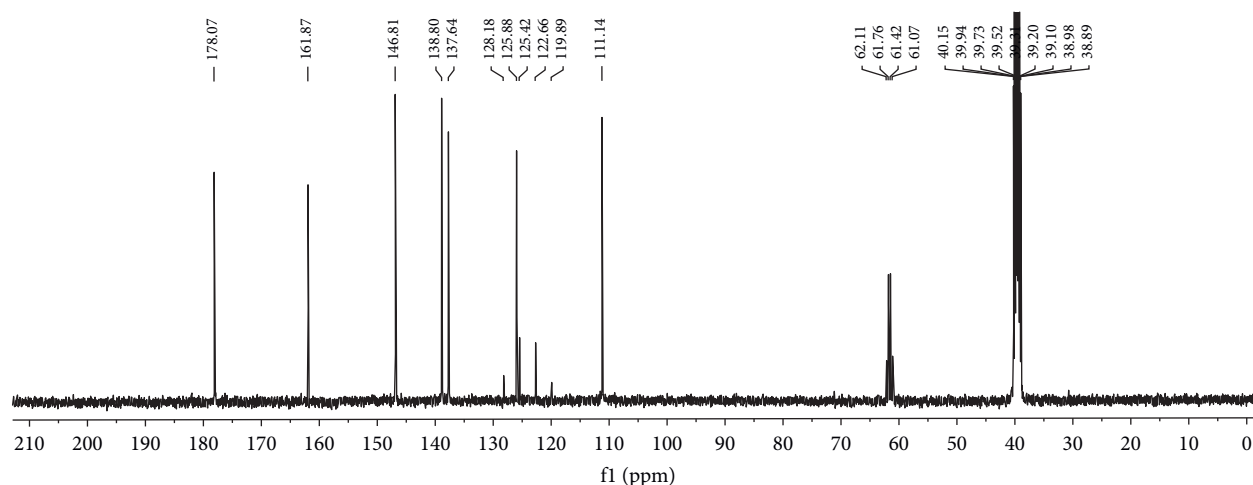


FIGURE 2: $^{13}\text{C}\{^1\text{H}\}$ NMR spectrum of compound 1.

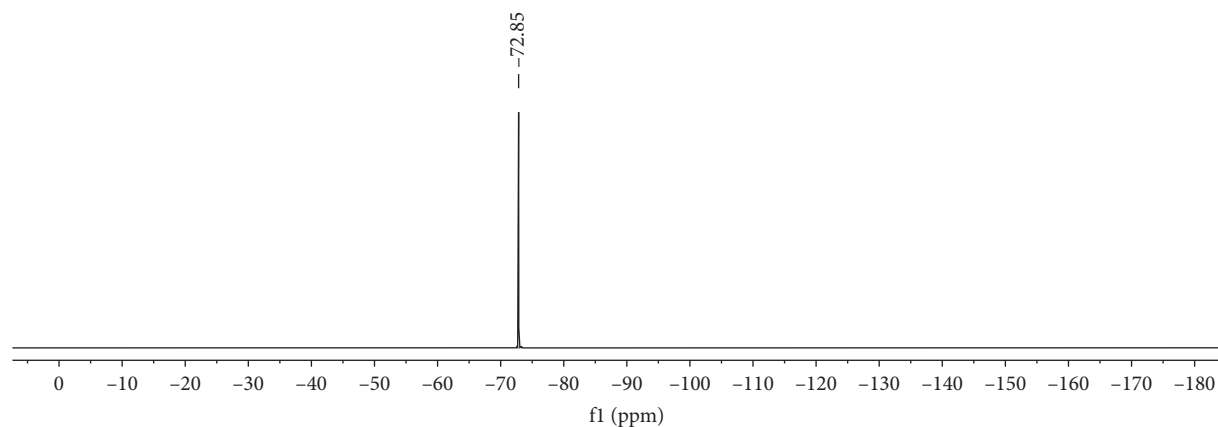


FIGURE 3: $^{19}\text{F}\{^1\text{H}\}$ NMR spectrum of compound 1.

positions C-2' (0.27, 0.39, and 0.84 ppm, for **2**, **5**, and **8**, respectively), C-4' (0.50 ppm for **8**), and C-6' (0.27, 0.15, and 0.84 ppm, for **2**, **5**, and **8**, respectively), while for **5** the signal of the proton in the position C-5' is shielded by 0.29 ppm, with respect to the unsubstituted phenyl moiety [23, 25].

In the ^{13}C -NMR spectra of compounds 1-8, the signals of the imine (C=N) carbon atoms appeared at $\delta = 149.40 - 135.48$. These results are similar to the chemical shifts found for the compounds (E)-N'-(pyridine-2-ylmethylene) azepane-1-carbothiohydrazide and 2-acetylpyridine-N(4)-1-(4-fluorophenyl)piperazinyl thiosemicarbazone ($\delta = 146.7$ and 148.48 , respectively) [33, 37]. The signals observed at $\delta = 178.98 - 171.65$ correspond to the thioamide carbons (C=S) [33, 38, 39]. The resonance lines of the pyridine carbons appeared at $\delta = 161.87 - 94.95$, and these chemical shifts are in agreement with those found for 2-benzoylpyridine-N(4)-ortho-fluorophenyl thiosemicarbazone ($\delta = 124.96 - 151.18$) [7]. The aromatic carbons of the phenyl group in all synthesized thiosemicarbazones were observed at $\delta = 162.41 - 110.29$ [37].

All fluorine containing compounds **1**, **2**, and **6** showed ^{19}F NMR signals as expected to their respective chemical environment (CF_3 -R, F-Ph, F-Py) [40].

3.2. Description of the Crystal Structure of Compound 7. Good quality crystals of **7**, suitable for single crystal X-ray diffraction analysis, were obtained by slow evaporation from a concentrated reaction mixture in methanol. For the other compounds, only microcrystalline solids were obtained from acetone. **7** crystallizes with two different crystal shapes and different unit cells. Its molecular structure together with the atomic numbering scheme is shown in Figure 4. Crystal data and refinement results for both types of crystals are summarized in Table 1, and selected bond lengths, bond angles, and torsion angles are given in Table 2. The values in the right column of Table 1 belong to the plate-like crystals, which correspond to the major fraction (>90%) of crystals, while the values in the left column belong to the minor fraction of rod-like crystals. The bond lengths, bond angles, and torsion angles for **7**, shown in Table 2, are similar for both crystal shapes. As reported in Table 1, both crystal structures of **7** belong to the monoclinic system and space

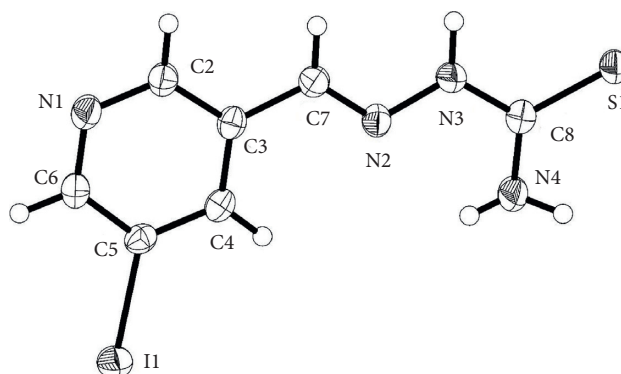


FIGURE 4: ORTEP diagram of 7 with thermal ellipsoids at the 50% probability level.

TABLE 1: Crystal and structure refinement data of 7 obtained as rod-like (left column) and plate-like crystals (right column).

Compound	7	
Empirical formula	C ₇ H ₇ IN ₄ S	
Formula weight	306.13	
Temperature (K)	180	
Wavelength (Å)	1.54186	
Crystal system	Monoclinic	
Space group	P2 ₁ /c	
a (Å)	8.8999(3)	9.6084(2)
b (Å)	4.5723(1)	7.9140(1)
c (Å)	24.7204(7)	14.0539(3)
α (°)	90	90
β (°)	94.444(2)	107.132(2)
γ (°)	90	90
Volume (Å ³)	1002.92(5)	1021.25(3)
Z	4	4
Density (calculated) (g/cm ³)	2.027	1.991
Absorption coefficient (mm ⁻¹)	26.720	26.241
F (000)	584	584
Crystal size (mm ³)	0.05 × 0.06 × 0.15	0.070 × 0.075 × 0.080
θ range for data collection (°)	3.5 to 70.6	4.8 to 70.6
Index ranges	-10 ≤ h ≤ 10 -5 ≤ k ≤ 2 -29 ≤ l ≤ 29	-11 ≤ h ≤ 11, -9 ≤ k ≤ 8, -17 ≤ l ≤ 10
Reflections collected	10874	18535
Independent reflections	1906 [R (int) = 0.029]	1961 [R (int) = 0.029]
Completeness to θ = 70.6°	98.8%	99.6%
Data/restraints/parameters	1906/0/140	1961/0/147
Goodness-of-fit on F ²	1.178	1.078
Final R indices (I > 2σ(I))	R1 = 0.0252, wR2 = 0.0635	R1 = 0.0274, wR2 = 0.0771
R Indices (all data)	R1 = 0.0265, wR2 = 0.0639	R1 = 0.0293, wR2 = 0.0780
Extinction coefficient	0.00051(7)	0.0003(1)
Largest diff. Peak and hole, e.Å ⁻³	0.69 and -0.50	0.97 and -0.74

group P2₁/c with one molecule in the asymmetric unit. Both types of crystals show the existence of the *E* conformation of the compound in the solid state.

The ORTEP diagram (Figure 4) reveals that 7 exists in the *E* conformation regarding the N2-N3 bond, as evidenced by the C7-N2-N3-C8 torsion angle of 177.0(4). This *E* conformation was also observed in other thiosemicarbazone derivatives [22, 25, 41, 42]. The bond distances observed for the C=N (C7-N2 1.280(5) Å) and

C=S (C8-S1 1.697(3) Å) groups are very close to the bond lengths found for the C=N (1.2831(18) and 1.2764(18) Å) and C=S (1.6786(14) and 1.6884(14) Å) groups, corresponding to compounds 2-formylpyridine-4-*N*-ethylthiosemicarbazone and (*E*)-2-(2-chlorobenzylidene)-*N*-methyl hydrazinocarbothioamide, respectively [22, 42]. These results confirm the existence of the thiosemicarbazone group in the thione form in the solid state. However, the N3-N2, N3-C8, C8-N4, and also the

TABLE 2: Selected bond distances (Å), bond angles ($^{\circ}$), and torsion angles ($^{\circ}$) of two different crystals, obtained for 7.

Distances*		Angles*		Torsion angles*	
N1-C2	1.338(5)	C7-N2-N3	116.4(3)	C3-C7-N2-N3	179.8(3)
	1.338(5)		114.5(3)		-179.1(3)
N1-C6	1.332(5)	C8-N3-N2	119.2(3)	C7-N2-N3-C8	177.2(4)
	1.342(5)		120.4(3)		177.0(4)
C7-N2	1.272(5)	N3-C8-S1	120.0(3)	C4-C3-C7-N2	1.7(6)
	1.280(5)		118.7(3)		-1.7(6)
N2-N3	1.378(5)	N3-C8-N4	117.9(4)	C2-C3-C7-N2	-178.1(4)
	1.367(5)		117.9(3)		179.4(4)
C8-N3	1.354(5)	N4-C8-S1	122.1(3)	N4-C8-N3-N2	4.1(6)
	1.348(5)		123.4(3)		4.3(5)
C8-S1	1.689(4)	N1-C2-C3	123.6(4)	C4-C5-C6-N1	-0.1(6)
	1.697(3)		124.2(4)		1.0(6)
C8-N4	1.325(5)	C6-C5-I1	118.3(3)	N1-C2-C3-C7	179.5(4)
	1.309(5)		118.2(3)		179.6(4)

*The first and second values of these bond parameters correspond to the minor and major fractions of crystals obtained for 7, respectively.

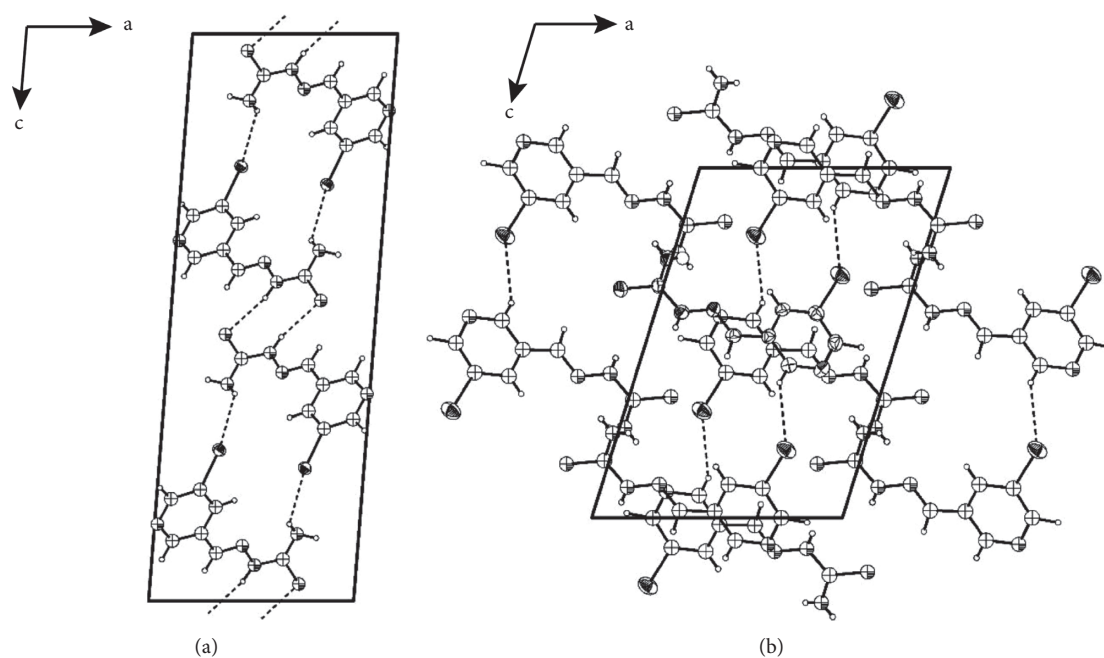


FIGURE 5: Packing diagrams of 7 in the rod-like (a) and plate-like (b) crystals.

C8-S1 bond distances are intermediate between the ideal values of corresponding double and single bonds. This indicates an extensive delocalized electron density on the N2-N3-C8-N4 chain [41, 42].

Accordingly, the C8-N3-N2 bond angles found for both crystal shapes (rod-like crystals: $119.2(3)^{\circ}$ and plate-like crystals: $120.4(3)^{\circ}$) of 7 are typical for sp^2 atoms. They are similar to those bond angles found for the N^4 -*ortho*, -*meta* and -*para*-fluorophenyl 2-acetylpyridine thiosemicarbazones (118.84, 118.67 and 119.18° , respectively). Weak intramolecular hydrogen bonds N2...H4-N4 contribute to the stability of the *E* conformation [43].

The tridentate (N, N, S) compound 7 deviates only slightly from planarity. The displacement from coplanarity is indicated by the dihedral angle between the pyridine ring and the plane defined by the C3-C7-N2-N3 chain; the values

being 1.8° for the rod-like crystals and 1.1° for the plate-like crystals. The packing of 7 in the rod-like crystals (Upper part of Figure 5) supports the fact that the molecules of 7 are involved in hydrogen bonds through the sulfur (thiocarbonyl) and the NH group of neighbouring moieties, S1...H3'-N3' (S1...H3' 2.44; S1...N3' 3.35 Å; S1...H3'-N3' 167° ; " : $1-x, 2-y, 1-z$). The shortest I...H distance is observed between the iodine (pyridinyl) atom I1 and the amine hydrogen atom H4b of a neighbouring molecule (I1...H4b" 3.21 Å; " : $1-x, y-0.5, 0.5-z$). In contrast, in the plate-like crystals of 7 (Lower part of Figure 5), the shortest intermolecular S...H distance is significantly longer (S1...H3' 2.80 Å; " : $-x, 2-y, 1-z$) and the shortest intermolecular I...H distance is slightly shorter (I1...H2" 3.13 Å; " : $x, 1.5-y, z-0.5$) than in the other crystalline form.

TABLE 3: IC₅₀ (μM) values^a of the pyridine-3-carbaldehyde thiosemicarbazone derivatives (1–8) against the 3T3 non-tumor cells and the different human tumor cell lines.

Comp.	Non-tumor cells				Tumor cells		
	3T3 ^b	H460	HuTu80	DU145	MCF-7	M-14	HT-29
5-FU ^c	<0.47	3.65 ± 0.81	3.68 ± 0.65	7.51 ± 0.98	2.45 ± 0.28	7.51 ± 0.73	4.54 ± 0.86
1	6.12 ± 0.33	10.90 ± 0.42	7.17 ± 0.35	21.35 ± 0.78	6.27 ± 0.24	3.36 ± 0.10	11.25 ± 0.41
2	>455.67	>455.67	>455.67	>455.67	>455.67	>455.67	>455.67
3	>582.26	>582.26	389.22 ± 10.42	582.26 ± 13.74	>582.26	>582.26	>582.26
4	60.49 ± 5.90	98.15 ± 4.12	40.00 ± 3.93	66.53 ± 2.46	73.17 ± 4.38	140.07 ± 1.90	232.35 ± 24.35
5	24.69 ± 2.45	52.95 ± 4.29	40.34 ± 3.56	43.04 ± 2.24	78.24 ± 4.92	>395.09	98.77 ± 6.73
6	537.24 ± 44.83	>537.24	215.47 ± 12.83	537.24 ± 14.04	348.36 ± 9.53	>537.24	537.24 ± 15.68
7	168.34 ± 6.36	254.79 ± 10.21	126.23 ± 9.74	183.09 ± 22.54	151.95 ± 9.12	102.08 ± 16.74	134.64 ± 10.51
8	>384.36	>384.36	>384.36	>384.36	>384.36	>384.36	>384.36

^aIC₅₀ corresponds to the concentration required to inhibit a 50% of the cell growth when the cells are exposed to the respective compound during 48 h. The values are mean ± standard deviation of two independent experiments. ^bMouse embryonic fibroblast cells. ^c5-fluorouracile.

3.3. Antitumor Evaluation. The synthesized compounds **1–8** were tested for their *in vitro* cytotoxic activity against the following six human tumor cell lines: large cell lung carcinoma (H460), duodenum adenocarcinoma (HuTu80), prostate carcinoma (DU145), breast adenocarcinoma (MCF-7), amelanotic melanoma (M-14), and colon adenocarcinoma (HT-29). For comparison purposes, the cytotoxicity of 5-fluorouracile (**5-FU**) was evaluated under the same experimental conditions, using the sulforhodamine B (SRB) assay [27]. The cytotoxicity of the compounds was calculated from their IC₅₀ values (the micromolar concentration of compound that inhibits 50% cell growth).

The antiproliferative activity of the thiosemicarbazones derivatives and 5-fluorouracile is shown in Table 3. The obtained results indicate that **1** was more cytotoxic (IC₅₀ = 3.36–21.35 μM) than the other tested thiosemicarbazones (IC₅₀ = 40.0–>582.26 μM) against all the tested cell lines. These results allow to confirm that the cytotoxic activity is enhanced when the OCH₂CF₃ substituent group is bound in the C-6 position of the pyridine ring [44]. As compared to the 5-fluorouracile (**5-FU**) anticancer agent (IC₅₀ = 7.51 μM), **1** exhibited a higher cytotoxic effect at low micromolar concentration (IC₅₀ = 3.6 μM) against the amelanotic melanoma cell line (M-14). In addition, **1** showed to be more innocuous (IC₅₀ = 6.12 μM) than **5-FU** (IC₅₀ = <0.47 μM) against the BALB/3T3 mouse embryo normal cells.

On the other hand, **5** (X = 3, 4-dimethoxyphenyl) showed a more acceptable cytotoxicity (IC₅₀ = 40.34–43.04 μM) than **8** (X = 3, 5-dichlorophenyl), with IC₅₀ values of >384.36 μM against the HuTu80 and DU145 cell lines. These results indicate that the presence of the methoxy substituent groups in the C-3 and C-4 positions of the benzene ring enhance the antitumor activity against these specific cell lines.

Compound **1** tested *in vitro* against the amelanotic melanoma cell line (M-14) (IC₅₀ = 3.36 μM) showed to be more cytotoxic as compared to pyridine-2-carbaldehyde thiosemicarbazone (IC₅₀ => 100 μM) assayed *in vitro* against the mouse metastatic skin melanoma (B16F10) cell line [44]. Nevertheless, **1** (IC₅₀ = 11.25 μM) tested *in vitro* against the colon adenocarcinoma (HT-29) was

slightly less active than pyridine-2-carbaldehyde thiosemicarbazone (IC₅₀ = 8.6 μM) and 2-acetylpyridine-N(4)-ortho-chlorophenyl thiosemicarbazone (IC₅₀ = 6.96 μM) assayed *in vitro* against the colon cancer (CT26.WT) and HT-29 cell lines, respectively [44, 45]. On the other hand, 3-aminepyridinecarbaldehyde thiosemicarbazone and 3-phenyl-1-pyridin-2-ylprop-2-en-1-one thiosemicarbazone tested *in vitro* against the large cell lung cancer (NCI-H460) [46] and the human breast carcinoma (MDA-MB 231) cell line [10], respectively, were found to be about two times more cytotoxic than **1** tested *in vitro* against the H460 and MCF-7 cell lines with IC₅₀ values of 10.9 and 6.27 μM, respectively. However, **1** (IC₅₀ = 6.27 μM) was more active than 4-phenyl-1-(quinoline-2-carbaldehyde) thiosemicarbazone (IC₅₀ => μM) [47] and diacetylpyridine bis(⁴N-tolylthiosemicarbazone) (IC₅₀ => 100 μM) assayed on the MCF-7 cell line [41]. In addition, **1** (IC₅₀ = 10.90 μM) tested on the H460 cell line showed higher cytotoxicity than 2-acetyl-pyridine thiosemicarbazone (IC₅₀ = 14.34 and 15.68 μM) and 4-methyl-1-(2-acetyl-pyridine) thiosemicarbazone (IC₅₀ = 11.10 and 15.53 μM) assayed against the NCI-H460 and MSTO-211H lung carcinoma cell lines, respectively [48].

The selectivity indexes which represent the ratio of the IC₅₀ values of the compounds on non-tumor cell line to those in the tumor cell line were calculated in order to determine if the pyridine-3-carbaldehyde thiosemicarbazone derivatives (**1–8**) were more cytotoxic on tumor cell lines compared with the 3T3 non-tumor cell line, and the results have been summarized in Table 4. Considering the low IC₅₀ values obtained for the tested compounds against the tumor and non-tumor cell lines, **1** displayed the highest selectivity index (SI = 1.82) against M-14 cell line as compared to those indexes observed for the other tested thiosemicarbazones and the 5-fluorouracile chemotherapeutic agent. This value means that compound **1** is 1.82 times more cytotoxic to the tumor cell line as compared to the 3T3 non-tumor cell line. This value can be considered as an acceptable selectivity index with respect to the highest selectivity index (2.81) found for the essential oil from *T. erecta* leaves against HT-29 tumor cell line and

TABLE 4: Selectivity of the cytotoxicity of the pyridine-3-carbaldehyde thiosemicarbazone derivatives (**1–8**) to tumor cells, as compared with 3T3 non-tumor cells.

Compound	Selectivity index ^a (SI)					
	H460	HuTu80	DU145	MCF-7	M-14	HT-29
5-FU ^b	<0.13	<0.13	<0.06	<0.19	<0.06	<0.10
1	0.56	0.85	0.29	0.98	1.82	0.54
2	NC	NC	NC	NC	NC	NC
3	NC	>1.50	1.00	NC	NC	NC
4	0.62	1.51	0.91	0.83	0.43	0.26
5	0.47	0.61	0.57	0.32	<0.06	0.25
6	<1.00	2.49	1.00	1.54	<1.00	1.00
7	0.66	1.33	0.92	1.11	1.65	1.25
8	NC	NC	NC	NC	NC	NC

^aThe selectivity index is the ratio of the IC₅₀ values of the compounds on 3T3 cells to those in the tumor cell lines. NC = unable to calculate. ^b5-Fluorouracile.

VT79 normal hamster lung fibroblast cells [49]. On the other hand, **6** displayed the highest selectivity indexes of 2.49 and 1.54 against HuTu80 and MCF-7 cell lines, respectively, with respect to the other tested thiosemicarbazone derivatives. However, the IC₅₀ values were very high (>200 μM) for both tumor cell lines.

Thus, it becomes evident that the studied thiosemicarbazones have a different activity depending on the substituents present in the respective structures. However, **2**, **3**, and **6**, even though the most innocuous compounds against the 3T3 normal cells do not present antitumor activity against the studied cell lines.

4. Conclusions

In this study, eight new pyridine-3-carbaldehyde thiosemicarbazone derivatives with different substituents were synthesized, characterized, and investigated for their antitumor activities. Only **7** gave good quality crystals for single crystal X-ray diffraction studies. The crystal structure of **7** exhibits an *E* conformation about the N2-N3 bond. This conformation was also assessed from solution ¹H NMR studies. The results of the cytotoxic assays and the selectivity indexes calculated demonstrated that compound **1** with IC₅₀ value of 3.36 μM and selectivity index of 1.82 has significant bioactivity towards amelanotic melanoma (M14) human tumor cell line. Therefore, **1** is a promising candidate as a pharmacological agent, since it presents significant activity and is more innocuous than the 5-fluorouracile anticancer drug against 3T3 mouse embryo fibroblast normal cells. Further studies are required to evaluate the mechanism of action for the anticancer activity of **1**.

Data Availability

The data used to support the findings of this study are included within the article. These data will be available when the researchers request it. Crystallographic data for the structural analyses have been deposited with the Cambridge Crystallographic Data Centre, numbers CCDC 1986928 and 1986929 for both forms of **7**. Copies of this information can be obtained free of charge via <http://www.ccdc.cam.ac.uk/>

conts/retrieving.html, or from the Cambridge Crystallographic Data Centre (CCDC, 12 Union Road, Cambridge CB2 1EZ, UK; fax (+44) 1223-336-033; e-mail: deposit@ccdc.cam.ac.uk).

Conflicts of Interest

The authors declare that they have no conflicts of interest.

Acknowledgments

The authors thank the Research Laboratory of the Faculty of Sciences and Philosophy, Universidad Peruana Cayetano Heredia, for the biological studies of the compounds and Miss Ramona Oehme of the Faculty of Chemistry and Mineralogy, Universität Leipzig, for the recording of mass spectra. WH thanks the Universidad de Lima Scientific Research Institute for financial support to carry out the research work. ES also thanks Financiamiento Basal Para Centros Científicos y Tecnológicos de Excelencia, AFB180001 (CEDENNA).

Supplementary Materials

Figure 6: FT-IR spectrum of **1**. Figure 7: Mass spectrum of **1**. Figure 8: Edited-HSQC spectrum of **1**. Figure 9: FT-IR spectrum of **2**. Figure 10: Mass spectrum of **2**. Figure 11: ¹H NMR spectrum (400 MHz, DMSO) of **2**. Figure 12: ¹³C NMR spectrum (100 MHz, DMSO) of **2**. Figure 13: Edited-HSQC spectrum of **2**. Figure 14: HMBC spectrum of **2**. Figure 15: FT-IR spectrum of **3**. Figure 16: Mass spectrum of **3**. Figure 17: ¹H NMR spectrum (300 MHz, DMSO) of **3**. Figure 18: ¹³C NMR spectrum (75 MHz, DMSO) of **3**. Figure 19: FT-IR spectrum of **4**. Figure 20: Mass spectrum of **4**. Figure 21: ¹H NMR spectrum (300 MHz, DMSO) of **4**. Figure 22: ¹³C NMR spectrum (75 MHz, DMSO) of **4**. Figure 23: FT-IR spectrum of **5**. Figure 24: Mass spectrum of **5**. Figure 25: ¹H NMR spectrum (300 MHz, DMSO) of **5**. Figure 26: ¹³C NMR spectrum (75 MHz, DMSO) of **5**. Figure 27: FT-IR spectrum of **6**. Figure 28 Mass spectrum of **6**. Figure 29 ¹H NMR spectrum (400 MHz, DMSO) of **6**. Figure 30: ¹³C NMR spectrum (75 MHz, DMSO) of **6**. Figure 31: ¹⁹F NMR spectrum (376 MHz, DMSO) of **6**. Figure 32: Edited-HSQC spectrum of **6**. Figure 33: HMBC spectrum of **6**. Figure 34:

FT-IR spectrum of 7. Figure 35: Mass spectrum of 7. Figure 36: ^1H NMR spectrum (300 MHz, DMSO) of 7. Figure 37: ^{13}C NMR spectrum (100 MHz, DMSO) of 7. Figure 38: HMBC spectrum of 7. Figure 39: FT-IR spectrum of 8. Figure 40: Mass spectrum of 8. Figure 41: ^1H NMR spectrum (400 MHz, DMSO) of 8. Figure 42: ^{13}C NMR spectrum (100 MHz, DMSO) of 8. (*Supplementary Materials*)

References

- [1] S. Padhyé and G. B. Kauffman, "Transition metal complexes of semicarbazones and thiosemicarbazones," *Coordination Chemistry Reviews*, vol. 63, pp. 127–160, 1985.
- [2] J. S. Casas, M. S. García-Tasende, and J. Sordo, "Main group metal complexes of semicarbazones and thiosemicarbazones. A structural review," *Coordination Chemistry Reviews*, vol. 209, no. 1, pp. 197–261, 2000.
- [3] S. A. Khan and A. M. Asiri, "Multi-step synthesis, spectroscopic studies of biological active steroidal thiosemicarbazones and their palladium(II) complex as macromolecules," *International Journal of Biological Macromolecules*, vol. 107, pp. 105–111, 2018.
- [4] A. Kolocouris, K. Dimas, C. Pannecouque et al., "New 2-(1-adamantylcarbonyl)pyridine and 1-acetyladamantane thiosemicarbazones-thiocarbonohydrazones: cell growth inhibitory, antiviral and antimicrobial activity evaluation," *Bioorganic & Medicinal Chemistry Letters*, vol. 12, no. 5, pp. 723–727, 2002.
- [5] Z. Zhong, B. Aotegen, H. Xu, and S. Zhao, "Structure and antimicrobial activities of benzoyl phenyl-thiosemicarbazone-chitosans," *International Journal of Biological Macromolecules*, vol. 50, no. 4, pp. 1169–1174, 2012.
- [6] A. B. M. Ibrahim, M. K. Farh, and P. Mayer, "Copper complexes of new thiosemicarbazone ligands: synthesis, structural studies and antimicrobial activity," *Inorganic Chemistry Communications*, vol. 94, pp. 127–132, 2018.
- [7] G. L. Parrilha, J. G. Da Silva, L. F. Gouveia et al., "Pyridine-derived thiosemicarbazones and their tin(IV) complexes with antifungal activity against *Candida* spp.," *European Journal of Medicinal Chemistry*, vol. 46, no. 5, pp. 1473–1482, 2011.
- [8] C. G. Oliveira, P. I. D. S. Maia, P. C. Souza et al., "Manganese(II) complexes with thiosemicarbazones as potential anti-*Mycobacterium tuberculosis* agents," *Journal of Inorganic Biochemistry*, vol. 132, pp. 21–29, 2014.
- [9] L. Sens, A. C. A. de Souza, L. A. Pacheco et al., "Synthetic thiosemicarbazones as a new class of *Mycobacterium tuberculosis* protein tyrosine phosphatase A inhibitors," *Bioorganic & Medicinal Chemistry*, vol. 26, no. 21, pp. 5742–5750, 2018.
- [10] J. G. Da Silva, A. A. Recio Despaigne, S. R. W. Louro, C. C. Bandeira, E. M. Souza-Fagundes, and H. Beraldo, "Cytotoxic activity, albumin and DNA binding of new copper(II) complexes with chalcone-derived thiosemicarbazones," *European Journal of Medicinal Chemistry*, vol. 65, pp. 415–426, 2013.
- [11] T. A. Yousef, G. M. Abu El-Reash, M. Al-Jahdali, and E.-B. R. El-Rakhawy, "Synthesis, spectral characterization and biological evaluation of Mn(II), Co(II), Ni(II), Cu(II), Zn(II) and Cd(II) complexes with thiosemicarbazone ending by pyrazole and pyridyl rings," *Spectrochimica Acta Part A: Molecular and Biomolecular Spectroscopy*, vol. 129, pp. 163–172, 2014.
- [12] J. Shao, Z.-Y. Ma, A. Li et al., "Thiosemicarbazone Cu(II) and Zn(II) complexes as potential anticancer agents: syntheses, crystal structure, DNA cleavage, cytotoxicity and apoptosis induction activity," *Journal of Inorganic Biochemistry*, vol. 136, pp. 13–23, 2014.
- [13] V. F. S. Pape, S. Tóth, A. Füredi et al., "Design, synthesis and biological evaluation of thiosemicarbazones, hydrazinobenzothiazoles and arylhydrazones as anticancer agents with a potential to overcome multidrug resistance," *European Journal of Medicinal Chemistry*, vol. 117, pp. 335–354, 2016.
- [14] J. Deng, P. Yu, Z. Zhang et al., "Designing anticancer copper(II) complexes by optimizing 2-pyridine-thiosemicarbazone ligands," *European Journal of Medicinal Chemistry*, vol. 158, pp. 442–452, 2018.
- [15] S. Datta, D. K. Seth, S. Gangopadhyay, P. Karmakar, and S. Bhattacharya, "Nickel complexes of some thiosemicarbazones: synthesis, structure, catalytic properties and cytotoxicity studies," *Inorganica Chimica Acta*, vol. 392, pp. 118–130, 2012.
- [16] K. O. Ferraz, S. M. S. V. Wardell, J. L. Wardell, S. R. W. Louro, and H. Beraldo, "Copper(II) complexes with 2-pyridineformamide-derived thiosemicarbazones: spectral studies and toxicity against *Artemia salina*," *Spectrochimica Acta Part A: Molecular and Biomolecular Spectroscopy*, vol. 73, no. 1, pp. 140–145, 2009.
- [17] K. Jayakumar, M. Sithambaresan, A. A. Aravindakshan, and M. R. P. Kurup, "Synthesis and spectral characterization of copper(II) complexes derived from 2-benzoylpyridine- N^4, N^4 -dimethyl-3-thiosemicarbazone: crystal structure of a binuclear complex," *Polyhedron*, vol. 75, pp. 50–56, 2014.
- [18] R. A. Finch, M.-C. Liu, S. P. Grill et al., "Triapine (3-aminopyridine-2-carboxaldehyde-thiosemicarbazone): a potent inhibitor of ribonucleotide reductase activity with broad spectrum antitumor activity," *Biochemical Pharmacology*, vol. 59, no. 8, pp. 983–991, 2000.
- [19] I. Gojo, M. L. Tidwell, J. Greer et al., "Phase I and pharmacokinetic study of triapine, a potent ribonucleotide reductase inhibitor, in adults with advanced hematologic malignancies," *Leukemia Research*, vol. 31, no. 9, pp. 1165–1173, 2007.
- [20] D. Kovala-Demertzi, P. N. Yadav, J. Wiecek, S. Skoulika, T. Varadinova, and M. A. Demertzis, "Zinc(II) complexes derived from pyridine-2-carbaldehyde thiosemicarbazone and (1E)-1-pyridin-2-ylethan-1-one thiosemicarbazone. Synthesis, crystal structures and antiproliferative activity of zinc(II) complexes," *Journal of Inorganic Biochemistry*, vol. 100, no. 9, pp. 1558–1567, 2006.
- [21] D. Kovala-Demertzi, A. Galani, N. Kourkoumelis, J. R. Miller, and M. A. Demertzis, "Synthesis, characterization, crystal structure and antiproliferative activity of platinum(II) complexes with 2-acetylpyridine-4-cyclohexyl-thiosemicarbazone," *Polyhedron*, vol. 26, no. 12, pp. 2871–2879, 2007.
- [22] D. Kovala-Demertzi, A. Galani, J. R. Miller, C. S. Frampton, and M. A. Demertzis, "Synthesis, structure, spectroscopic studies and cytotoxic effect of novel palladium(II) complexes with 2-formylpyridine-4-Nethyl-thiosemicarbazone: potential antitumor agents," *Polyhedron*, vol. 52, pp. 1096–1102, 2013.
- [23] W. Hernández, J. Paz, A. Vaisberg, E. Spodine, R. Richter, and L. Beyer, "Synthesis, characterization, and in vitro cytotoxic activities of benzaldehyde thiosemicarbazone derivatives and their palladium(II) and platinum(II) complexes against various human tumor cell lines," *Bioinorganic Chemistry and Applications*, vol. 2008, Article ID 690952, 9 pages, 2008.

- [24] W. Hernández, J. Paz, F. Carrasco et al., "Synthesis and characterization of new palladium(II) complexes with ligands derived from furan-2-carbaldehyde and benzaldehyde thiosemicarbazone and their in vitro cytotoxic activities against various human tumor cell lines," *Zeitschrift für Naturforschung B*, vol. 65, no. 10, pp. 1271–1278, 2010.
- [25] W. Hernández, J. Paz, F. Carrasco et al., "Synthesis and characterization of new palladium(II) thiosemicarbazone complexes and their cytotoxic activity against various human tumor cell lines," *Bioinorganic Chemistry and Applications*, vol. 2013, Article ID 524701, 12 pages, 2013.
- [26] W. Hernández, A. J. Vaisberg, M. Tobar et al., "In vitro antiproliferative activity of palladium(ii) thiosemicarbazone complexes and the corresponding functionalized chitosan coated magnetite nanoparticles," *New Journal of Chemistry*, vol. 40, no. 2, pp. 1853–1860, 2016.
- [27] P. Skehan, R. Storeng, D. Scudiero et al., "New colorimetric cytotoxicity assay for anticancer-drug screening," *Journal of the National Cancer Institute*, vol. 82, no. 13, pp. 1107–1112, 1990.
- [28] Stoe & Cie GmbH, X-Area 1.87, Software Package for Collecting Single-Crystal Data on STOE Area-Detector Diffractometers, for Image Processing, Scaling Reflection Intensities and for Outlier Rejection, Darmstadt, Germany, 2019.
- [29] G. M. Sheldrick, "A short history of SHELX," *Acta Crystallographica Section A Foundations of Crystallography*, vol. 64, no. 1, pp. 112–122, 2008.
- [30] K. Brandenburg, *Diamond-Crystal and Molecular Structure Visualization-Version 3.2k*, Crystal Impact GBr, Bonn, Germany, 2014.
- [31] R. K. Agarwal, L. Singh, and D. K. Sharma, "Synthesis, spectral, and biological properties of copper(II) complexes of thiosemicarbazones of schiff bases derived from 4-aminoantipyrine and aromatic aldehydes," *Bioinorganic Chemistry and Applications*, vol. 2006, Article ID 59509, 10 pages, 2006.
- [32] P. F. Rapheal, E. Manoj, and M. R. P. Kurup, "Syntheses and EPR spectral studies of manganese(II) complexes derived from pyridine-2-carbaldehyde based N(4)-substituted thiosemicarbazones: crystal structure of one complex," *Polyhedron*, vol. 26, no. 17, pp. 5088–5094, 2007.
- [33] D. Kovala-Demertzi, A. Papageorgiou, L. Papathanasis et al., "In vitro and in vivo antitumor activity of platinum(II) complexes with thiosemicarbazones derived from 2-formyl and 2-acetyl pyridine and containing ring incorporated at N(4)-position: synthesis, spectroscopic study and crystal structure of platinum(II) complexes with thiosemicarbazones, potential anticancer agents," *European Journal of Medicinal Chemistry*, vol. 44, no. 3, pp. 1296–1302, 2009.
- [34] R. Manikandan, P. Vijayan, P. Anitha et al., "Synthesis, structure and in vitro biological activity of pyridoxal N(4)-substituted thiosemicarbazone cobalt(III) complexes," *Inorganica Chimica Acta*, vol. 421, pp. 80–90, 2014.
- [35] D. C. Reis, M. C. X. Pinto, E. M. Souza-Fagundes, S. M. S. V. Wardell, J. L. Wardell, and H. Beraldo, "Antimony(III) complexes with 2-benzoylpyridine-derived thiosemicarbazones: cytotoxicity against human leukemia cell lines," *European Journal of Medicinal Chemistry*, vol. 45, no. 9, pp. 3904–3910, 2020.
- [36] P. Sengupta, R. Dinda, S. Ghosh, and W. S. Sheldrick, "Synthesis and characterization of some biologically active ruthenium(II) complexes of thiosemicarbazones of pyridine 2-aldehyde and thiophene 2-aldehyde involving some ring substituted 4-phenylthiosemicarbazides and 4-cyclohexylthiosemicarbazide. Crystal structure of $cis-[Ru(PPh_3)_2(L^6H)_2](ClO_4) \cdot 2 \cdot 2H_2O$ [$L^6H=4$ -(cyclohexyl) thiosemicarbazone of pyridine 2-aldehyde]," *Polyhedron*, vol. 22, no. 3, pp. 447–453, 2003.
- [37] T. P. Stanojkovic, D. Kovala-Demertzi, A. Primikyri et al., "Zinc(II) complexes of 2-acetyl pyridine 1-(4-fluorophenyl)-piperazinyl thiosemicarbazone: synthesis, spectroscopic study and crystal structures - potential anticancer drugs," *Journal of Inorganic Biochemistry*, vol. 104, no. 4, pp. 467–476, 2010.
- [38] O. Abdalla, Y. Farina, and N. Ibrahim, "Synthesis, characterization and antibacterial study of copper(II) complexes of thiosemicarbazones," *Malaysian Journal of Analytical Sciences*, vol. 19, pp. 1171–1178, 2015.
- [39] B. Şen, H. K. Kalhan, V. Demir, E. E. Güler, H. A. Kayal, and E. Subaş, "Crystal structures, spectroscopic properties of new cobalt(II), nickel(II), zinc(II) and palladium(II) complexes derived from 2-acetyl-5-chloro thiophene thiosemicarbazone: anticancer evaluation," *Materials Science and Engineering: C*, vol. 98, pp. 550–559, 2018.
- [40] S. Berger, S. Braun, and H. O. Kalinowski, *NMR Spectroscopy of the Non-Metallic Elements*, Wiley, Chichester, UK, 1997.
- [41] A. I. Matesanz, I. Leitao, and P. Souza, "Palladium(II) and platinum(II) bis(thiosemicarbazone) complexes of the 2,6-diacetylpyridine series with high cytotoxic activity in cisplatin resistant A2780cisR tumor cells and reduced toxicity," *Journal of Inorganic Biochemistry*, vol. 125, pp. 26–31, 2013.
- [42] K. Sampath, S. Sathiyaraj, and C. Jayabalakrishnan, "DNA binding, DNA cleavage, antioxidant and cytotoxicity studies on ruthenium(II) complexes of benzaldehyde 4-methyl-3-thiosemicarbazones," *Spectrochimica Acta Part A: Molecular and Biomolecular Spectroscopy*, vol. 105, pp. 582–592, 2013.
- [43] M. A. Soares, J. A. Lessa, I. C. Mendes et al., " N^4 -Phenyl-substituted 2-acetylpyridine thiosemicarbazones: cytotoxicity against human tumor cells, structure-activity relationship studies and investigation on the mechanism of action," *Bioorganic & Medicinal Chemistry*, vol. 20, no. 11, pp. 3396–3409, 2012.
- [44] T. T. Tavares, G. C. Azevedo, A. Garcia et al., "Gold(I) complexes with aryl-thiosemicarbazones: molecular modeling, synthesis, cytotoxicity and TrxR inhibition," *Polyhedron*, vol. 132, pp. 95–104, 2017.
- [45] G. L. Parriha, K. S. O. Ferraz, J. A. Lessa et al., "Metal complexes with 2-acetylpyridine- $N(4)$ -orthochlorophenylthiosemicarbazone: cytotoxicity and effect on the enzymatic activity of thioredoxin reductase and glutathione reductase," *European Journal of Medicinal Chemistry*, vol. 84, pp. 537–544, 2014.
- [46] J. Qi, J. Deng, K. Qian et al., "Novel 2-pyridinecarboxaldehyde thiosemicarbazones Ga(III) complexes with a high antiproliferative activity by promoting apoptosis and inhibiting cell cycle," *European Journal of Medicinal Chemistry*, vol. 134, pp. 34–42, 2017.
- [47] Y. Gou, J. Wang, S. Chen et al., " α - N -heterocyclic thiosemicarbazone Fe(III) complex: characterization of its antitumor activity and identification of anticancer mechanism," *European Journal of Medicinal Chemistry*, vol. 123, pp. 354–364, 2016.
- [48] J. Qi, Y. Zheng, K. Qian et al., "Synthesis, crystal structure and antiproliferative mechanisms of 2-acetylpyridine-thiosemicarbazones Ga(III) with a greater selectivity against tumor cells," *Journal of Inorganic Biochemistry*, vol. 177, pp. 110–117, 2017.
- [49] P. F. de Oliveira, J. M. Alves, J. L. Damasceno et al., "Cytotoxicity screening of essential oils in cancer cell lines," *Revista Brasileira de Farmacognosia*, vol. 25, no. 2, pp. 183–188, 2015.